Nanoscale

Accepted Manuscript

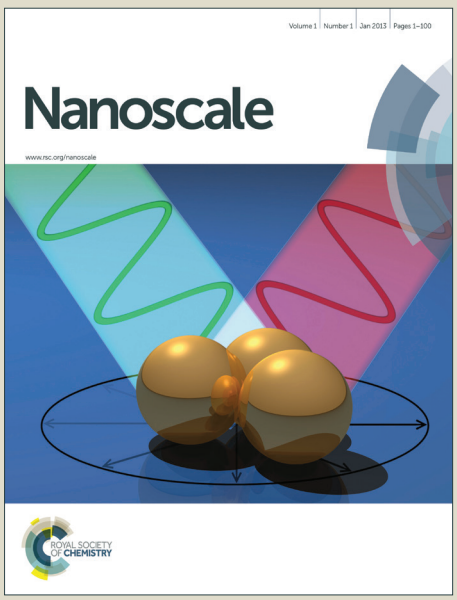

ROYAL SOCIETY OF CHEMISTRY

www.rsc.org/nanoscale

Journal Name

RSCPublishing

ARTICLE

Single Layer Lead Iodide: Computational Exploration of Structural, Electronic and Optical Properties, Strain induced Band Modulation and the Role of Spin-orbital-Coupling

giCite this: DOI: 10.1039/x0xx00000x

Received 00th January 2012,
Accepted 00th January 2012

DOI: 10.1039/x0xx00000x

www.rsc.org/

Mei Zhou[a], Wenhui Duan[a,d,*], Ying Chen[b], Aijun Du[c,*],

Graphitic like layered materials exhibit intriguing electronic structures and thus the search for new types of two-dimensional (2D) monolayer materials is of great interest for developing novel nano-devices. By using density functional theory (DFT) method, here we for the first time investigate the structure, stability, electronic and optical properties of monolayer lead iodide (PbI_2). The stability of PbI_2 monolayer is first confirmed by phonon dispersion calculation. Compared to the calculation using generalized gradient approximation, screened hybrid functional and spin-orbit coupling effects can not only predicts an accurate bandgap (2.63 eV), but also the correct position of valence and conduction band edges. The biaxial strain can tune its bandgap size in a wide range from 1 eV to 3 eV, which can be understood by the strain induced uniformly change of electric field between Pb and I atomic layer. The calculated imaginary part of the dielectric function of 2D Graphene/PbI_2 van der Waals type hetero-structure shows significant red shift of absorption edge compared to that of a pure monolayer PbI_2. Our findings highlight a new interesting 2D material with potential applications in nanoelectronics and optoelectronics.

Introduction

Two-dimensional (2D) layered crystal materials, such as graphene, [1] silicene, [2, 3] germanene, [4-6] hexagonal boron nitride, [7] and transition metal dichalcogenides [8-10] and black phosphorus, [11] have attracted intensive research efforts due to their remarkable electronic properties and potential applications in the miniature electronics in recent years [12-17]. Such 2D materials have been theoretically predicted and experimentally confirmed to possess novel properties which are different from or even better than their bulk counterparts. Up to now, a diverse range of intriguing properties of 2D materials have been revealed, highlighting the potential applications in energy, photonics and nano-electronics. However, the practical application based on the above 2D materials have serious band gap hurdles, i.e. the lack of obvious gap in graphene [1] and too large gap in boron nitride[7]. Single layer metal di-chalcogenides such as MoS_2 possess an appropriate band gap, but are strongly influenced by metal contacts, interface traps, charged impurities, dielectric environment, and structural defects. [10] Therefore the search for new types of 2D structures with proper band gaps is of paramount importance for next generation nano-device fabrication.

Lead iodine (PbI_2) is a metal halide that adopts the layered CdI_2 structural type. [18] The stacking order in an individual 2D PbI_2 layer is ABC rather than ABA. Several ordered polytypes of

PbI_2 exist, [18-20] of which the most common polytype is 2H form (a= 4.56 Å, c= 6.99 Å), which is the most stable form when the PbI_2 crystals are grown at room temperature. Bulk PbI_2 is a direct band gap semiconductor with an energy gap around 2.5 eV [21-26] with important applications as a room temperature detector material for both γ- and X-radiation. [27-29] In addition, PbI_2 has been reported to be a good candidate for thin film transistors and can serve as precursor for the organo lead iodide perovskites employed in high efficient hybrid solar cells[30-33]. Various forms of PbI_2 including thin films, nano-clusters, multiwalled nanotubes of lead iodide have been experimentally explored[34-38]. The successful growth of single-layered PbI_2 nanotubes within the carbon nanotubes was reported in most recent experiment[39]. Up to now, no theoretical research has been conducted in the single layer PbI_2 nano-sheet regarding its structure, stability, electronic and optical properties. Strain has demonstrated to have remarkable effect in tailoring electronic, optical and transport properties of 2D semiconductors [40, 41] and a full analysis of the strain effect on the band gap and electronic structure of single layer PbI_2 is highly desired. Additionally, spin-orbital-coupling[42] in bulk PbI2 modifies the band gap 0.85 eV[26], which is about 1/3 of band gap. Thus, it is also expected to be significant in the monolayer PbI2 and is worth exploring. Hybrid PbI_2 and carbon nanotube complex has been experimentally realized and an in-depth understanding of its electronic and optical properties is critical for future development of photonics device based on monolayer PbI_2.

In this paper, we have systematically investigated structure, stability, electronic and optical properties, and the effect of strain and spin-orbital-coupling in monolayer PbI_2. The stability is first confirmed by phonon dispersion. Our results show that monolayer PbI_2 is an indirect semiconductor with a predicted band gap of 2.63 eV. The band gap of monolayer PbI_2 can be substantially tuned from 1 eV to 3 eV. Spin orbit coupling is significant, giving rise to a bandgap reduction of 0.71 eV. Most interestingly, interfacing electrically active graphene and single layer PbI_2 form a 2D van der Waals type hetero-structure that can significant enhance the visible light response, suggesting potential applications in optoelectronics and photovoltaics.

Computational Methods

All calculations were carried out using the Vienna Ab-initio Simulation Package (VASP) codes [43,44]. The Perdew-Burke-Ernzerhof (PBE)[45] generalized gradient approximation (GGA) exchange correlation functional with the projector-augmented wave (PAW) [46,47] methods were used for geometry optimization. Hybrid functional methods based on Heyd-Scuseria-Ernzerhof (HSE06) method [48, 49] were adopted to correct the intrinsic band problem in DFT[50-53]. In the HSE06 method, a fraction of the exact screened Hartree–Fock (HF) exchange is incorporated into the PBE exchange using a mixing parameter α = 0.25. The energy cut-off for the plane wave basis was set to 400 eV. A Monkhorst-Pack k-point mesh 9×9×1 and 41×41×1, was used to sample the two dimensional Brillouin zone for geometry optimization and density of states calculation respectively. The corresponding k-point mesh used for bulk calculation were 11×11×7 and 15×15×11, respectively. The criterion for energy convergence was 10^{-6} eV. The atomic positions were fully relaxed until the residual Hellmann−Feynman force per atom converges to less than 0.01 eV/Å. The vacuum space is around 20 Å, which is enough to avoid the interaction between periodical images. The spin−orbit coupling effect is also considered in the calculation. Phonon dispersion was carried out using the Phonopy[54] code interfaced with the VASP code. In phonon calculations, a more stringent convergence criterion (10^{-8} eV for total energy and 10^{-4} eV/Å for Hellmann-Feynman Force) was employed. The frequency-dependent dielectric matrix was calculated for monolayer PbI_2 and the hybrid Graphene/PbI_2 structure. The long range van der Waals (vdW) interaction between monolayer PbI2 and Graphene is accounted by zero damping DFT-D3 method of Grimme.[55] The imaginary part was determined by a summation over empty states using the equation: [56]

$$\varepsilon^{n}_{\alpha\beta}(\omega)=\frac{4\pi^2e^2}{\Omega}\lim_{q\to 0}\frac{1}{q^2}\sum_{c,v,k}2\omega_k\delta(\varepsilon_{ck}-\varepsilon_{vk}-\omega)\times\left\langle\mu_{ck+e_{\alpha q}}\middle|\mu_{vk}\right\rangle\left\langle\mu_{ck+e_{\alpha q}}\middle|\mu_{vk}\right\rangle^{*}$$

where the indices c and v represent conduction (CB) and valence band (VB) states, respectively, and μ_{ck} refers to the cell periodic part of the orbitals at the k-point. A large number of empty CB states (128 bands, four times occupied bands in our calculations) will be included for accurate summation in eq 1.

Results and Discussions

The single layer PbI_2 nanosheet takes a buckled honeycomb structure, in which a layer of Pb atoms is sandwiched between two layers of I-atoms (schematic representation in Fig. 1 (a) and (b), respectively). Each Pb atom is surrounded by 6 I-atoms forming a near-octahedral $[PbI_6]^{4-}$ unit, which is condensed to layers by sharing edges with six neighbouring octahedra. Our initial configuration of the monolayer PbI_2 was obtained from the 2H phase PbI_2 (P3m1).[18] The optimized lattice constant and height of single layer PbI_2, i.e. the distance between top and bottom I-Pb atom layers are 4.66 Å and 3.72 Å respectively, which are in good agreement with the experimental bulk values[39]. Before the detailed electronic structure investigations, we firstly examine the dynamic stability of monolayer PbI_2 by calculating its phonon band structure and the corresponding result is displayed in Fig. 1 (c). We also provide phonon spectrum of single layer PbI_2 with the polarity taken into account in Fig. S1. More discussions about phonon mechanical stability of monolayer PbI_2 can be seen in the supporting information. Clearly, all phonon modes are positive, confirming that the quasi-two dimensional PbI_2 monolayer is dynamically stable.

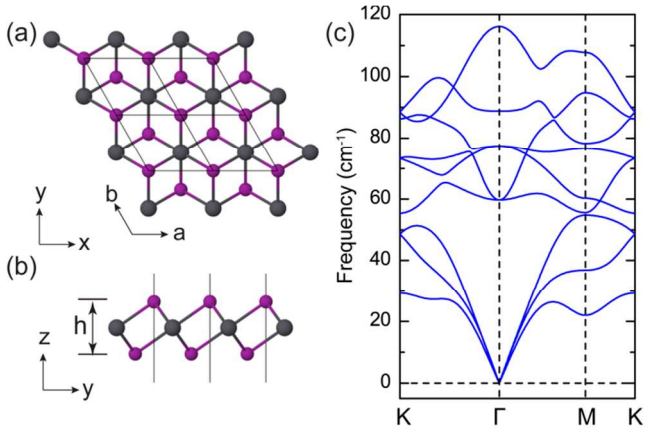

FIG. 1. (color online) (a) and (b) Top and side view of the atomic structure of monolayer PbI_2. (grey: lead, purple: iodine) The studied unit cell is indicated with black dashed rhombus. Lattice constant is labelled with a/b while the height due to buckled configurations is marked with h. (c) The phonon dispersion of monolayer PbI_2.

With the optimized monolayer PbI_2 and confirmed dynamic stability, we now turn to study its electronic structure. Fig. 2 (a) presents the electronic band structure of monolayer PbI_2 obtained with the PBE functional. Bulk PbI_2 is reported to be a direct band gap semiconductor of which the smallest gap appears at the surface of the Brillouin zone at points A[57], which also has been confirmed by our calculations (see Fig. S2). In single layer PbI_2, the original A (H and L) point of bulk Brillouin zone folds back to Γ (K and M) point, so that the original A-H and A-L directions project onto the Γ-K and Γ-M directions of monolayer. While the conduction band minimum (CBM) is still located at Γ point, the valence band maximum (VBM) shifts away from Γ point. Results from our calculations confirm that the VBM transfers about 1 / 3 away from Γ point. Therefore, monolayer PbI_2 becomes an indirect semiconductor with a band gap Δ_2 of 2.51 eV, which is about 0.37 eV smaller than direct band gap Δ_1. Together with CB and VB, we define another two VBs of monolayer PbI_2 (labelled as VB_{-1}, and VB_{-2}) around the Fermi level as shown in Fig. 2 (a).

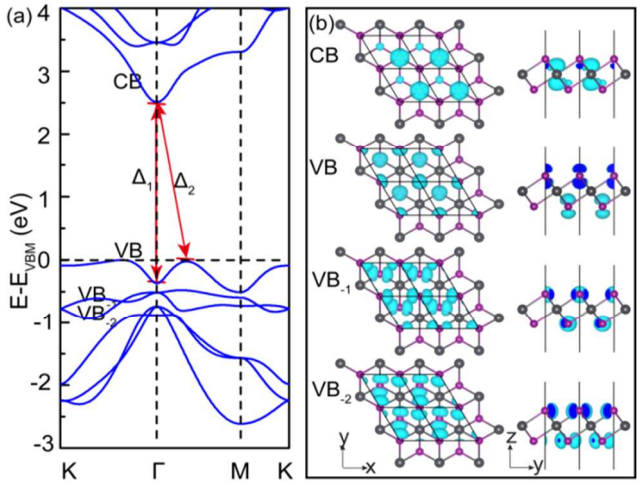

FIG. 2. (colour online) Electronic structure of the monolayer PbI_2. (a) Band structure of monolayer PbI_2 calculated with PBE functional. One conduction state (CB) and three valence states (VB, VB_{-1}, and VB_{-2}) are marked in the panel (a). Δ_1 and Δ_2 denotes direct and indirect band gap respectively. (b) Partial charge density plots for the four marked states of monolayer PbI_2 at Γ point illustrated in the xy and yz planes with an isosurface of 0.05 e/Å^{-3}. (grey: lead, purple: iodine)

In order to obtain more information on the change of states near the Fermi level, band-decomposed charge density of these four bands are calculated at Γ point as depicted in Fig. 2 (b) . Similar to bulk PbI_2[57-59], p orbitals dominate the CB and VB states of monolayer PbI_2. More detailed analysis revealed that 6 p_z like orbitals of lead contribute mainly to the conduction band and $5p_z$ orbitals of iodine and 6s orbitals of lead contribute to the

valence band VB. Unlike the mixed features of CB and VB, VB_{-1}, and VB_{-2} contain pure $5p_x$ orbitals and $5p_y$ orbitals from iodine, respectively. From bulk to quasi two dimensional PbI_2, the most significant change goes to iodine atoms due to their special positions in the layers, while strong effect from neighbouring layers is gone. Thus, this confinement effects that affect valance bands with contribution mainly from iodine atoms at A point tune PbI_2 from a direct band gap in bulk form to an indirect band gap semiconductor in 2D monolayer form.

It is important to note that the spin-orbital coupling (SOC) interaction in heavy elemental Pb (0.89 eV)[60] and I (0.95 eV) [61] atoms and bulk PbI_2[26] are significant. Therefore, it is expected to be vital in monolayer PbI_2 and need to be included. In fact, as depicted in Fig. 3 (a) and (b), the presence of SOC substantially lowers CBM by 0.60 eV and raises the VBM by 0.11 eV using the PBE functional, thereby reducing the band gap of monolayer PbI_2 up to 1.80 eV. Compare to bulk PbI_2 (see Supporting Information), the spin orbit coupling energy doesn't change too much. The standard PBE functional is well known to underestimate the bandgap of monolayer PbI_2, but the bandgap can be partially corrected by the screened hybrid HSE06 functional. Fig. 3 (c) displays band structure of monolayer PbI_2 calculated by using HSE06 functional and incorporating SOC effect. Compared to the PBE calculation with SOC (see Fig. 3a and 3b), HSE06 functional raises the CBM about 0.28 eV and lowers the VBM 0.55 eV, amending the band gap to 2.63 eV. Although the PBE calculation without SOC effect predicts a similar gap (2.51 eV) as obtained with the HSE06 functional and SOC interaction, the energy level of CBM and VBM are fully incorrect as illustrated in Fig. 3(d), potential leading to qualitative errors when predicting the position of defect energy level, band alignment and optical properties. Such an effect has been recently reported in a similar system, i.e. lead organic-inorganic lead iodide prevoskite solar cell materials[62]. Therefore, the use of HSE06 functional and spin orbit-coupling correction is important in obtaining the accurate electronic structure in monolayer PbI_2.

We also provide theoretical predictions for the charge carrier mobility of monolayer PbI_2. In order to calculate the carrier mobility, we construct a supercell $\sqrt{3} \times 1$ with $a = 8.07$ Å, $b = 4.66$ Å as shown in Fig. S5 (a) (red dash rectangle). The predicted carrier mobility of monolayer PbI_2 is generally not very large, but asymmetric between electrons and holes, where electrons are more mobile than holes in both x and y directions. The electron mobility along the x direction is estimated to be 122.22 $cm^2V^{-1}s^{-1}$, which is comparable to that of monolayer MoS_2 (~217 $cm^2V^{-1}s^{-1}$)[63] and Si thin film (~121 $cm^2V^{-1}s^{-1}$)[64]. The details of discussions and method can be found in Supporting Information.

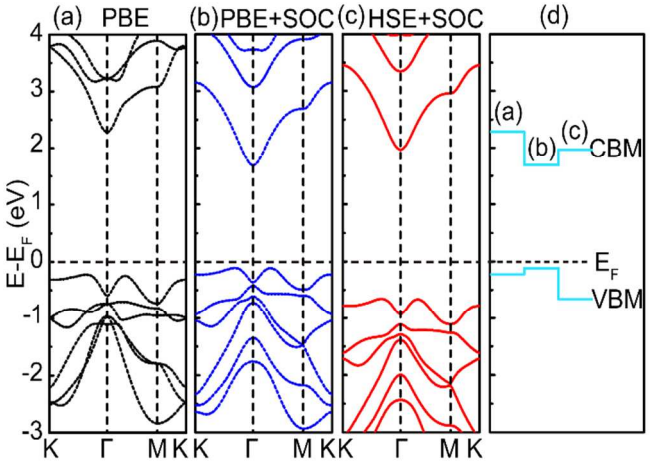

FIG. 3. (color online) Electronic structure of monolayer PbI_2 calculated with PBE functional without (a) and with (b) spin-orbit coupling effect (PBE+SOC), HSE06 functional with (c) spin-orbit coupling effect (HSE+SOC) , respectively. (d) CBM and VBM calculated using PBE, PBE+SOC, and HSE+SOC calculations.

Now we turn to study the strain effect on the electronic structure of monolayer PbI_2. Various lattice parameters along lattice vector of a/b direction are chosen. A biaxial strain is defined as $\varepsilon = \Delta a/a_0$, where a_0 is the equilibrium lattice constant at zero strain and Δa is the difference between the frozen and optimized lattice constant along lattice vector a/b direction, respectively. The positive and negative values of strain correspond to lattice expansion and compression, respectively. Starting with the fully relaxed PbI_2, we choose strain within the range of ± 20% to explore its effect on the band gap modulation. According to our calculations, the minimum of the bond between I and Pb in monolayer PbI_2 under various strains is larger than the sum of outmost cutoff radius of I and Pb atoms in the PBE pseudopotential, which suggests the results obtained from this pseudopotential for PbI_2 can be seen as reliable. (More discussions can be found in Supporting Information) In order to study the mechanical stability of PbI_2 under biaxial

strain, we have calculated a stress-strain curve as shown in Fig. S4 with a strain ranging from -25% to 25%. Our results clearly indicated that the 2D PbI_2 layers could sustain 10-20% strain. Since the elastic strain limit of graphene has been demonstrated to be around 20% by experimental results[65] and that of the single layer TMDs (transition metal dichalcogenides) is about 11%[66,67], we can expect that the critical strain of monolayer PbI_2 bears can also be realized by experiment in the near future. (More discussions can be seen in Supporting Information).

As depicted in Fig. 4, the calculations with the PBE functional predicted a linear decrease of band gap with increasing tensile strain. The band gap increases continually as a function of compressive strain and reaches up to the maximum at a strain of around -8%, after which drops sharply. Including the spin orbit interaction and the correction from the HSE06 functional, we obtain more accurate band gap in monolayer PbI_2 as a function of strain shown in Fig. 4. Obviously, the general trends of biaxial strain effects on the band gap variation of monolayer PbI_2 is similar, irrespective of the choice of functional and the inclusion of SOC effects. It should be also noted that the band gap of monolayer PbI_2 can be greatly modulated even at a compressive/tensile strain up to 20%. However, monolayer PbI_2 is elastic and mechanically stable only when the strain value is within 10% according to our calculation. A wide range band gap value of monolayer PbI_2 (1-3 eV) can still be obtained when strain changed from -10% to +10%. A desirable gap might be obtained in single layer PbI_2 for potential electronics and optoelectronics application by applying moderate biaxial strain.

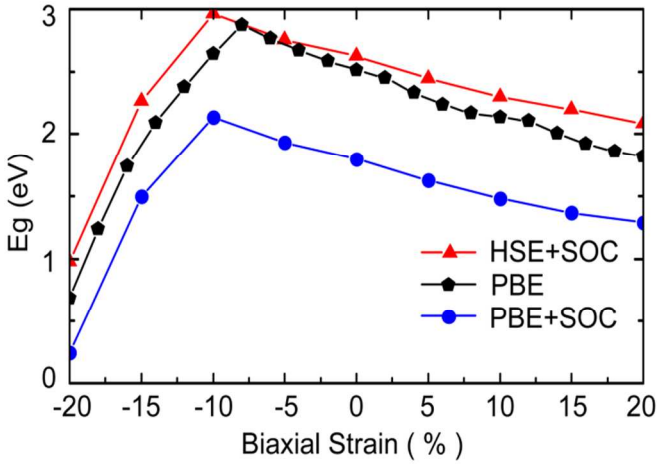

FIG. 4. (color online) Band gap of single layer PbI_2 as a function of biaxial strain predicted by PBE (blue circle) and HSE06 (red triangle) with spin orbit coupling effect, PBE calculations without orbit coupling effect (black pentagon).

Fig. 5 presents the band structure of monolayer PbI_2 at various strains. It can be seen clearly that increasing tensile strain reduces the width of CB notably and shifts down the position of CBM. In contrast with CBM, the VBM shifts about 1 / 3 away from Γ point to K point (after 5%) and then to M point (after 15%). As a result, the monolayer PbI_2 still remains to be an indirect gap semiconductor. In the case of compressive strain, both CBs and VBs can be significantly changed. The CBM is pushed up before the strain of -10% but VBM is slightly changed, leading to a wider band gap for single layer PbI_2. After the critical strain of -10%, the CBM transfers to M point, while the VBM is moving towards Γ point. Increasing compressive strain induces large dispersion for both CBs and VBs and the pull-back of CBM towards the Fermi level. Consequently, the band gap of monolayer PbI_2 reduces, but still remains to be indirect.

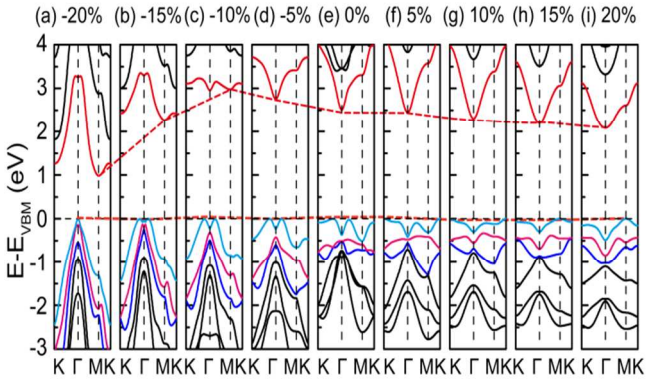

FIG 5. (color online) (a-i) Hybrid functional HSE06 predicted band structures of PbI_2 with different values of biaxial strain with spin orbit coupling effect. Red dashed lines are guide for viewing the energy shifts of VBM and CBM. (solid lines: red: CB, ball blue: VB, bright pink: VB_{-1}, blue: VB_{-2})

Further analysis indicated that the bond length between Pb and I atoms is nearly unchanged, but the height of monolayer PbI_2 increases linearly with the decreasing biaxial strain from tensile to compressive. In a single layer PbI_2 nanosheet,[68] the lead ions sit at a strong electric field induced by the tightly bound negative iodine ions on each side. Based on the assumption that there exists an electric field between Pb and I layers, the

increasing height will lead to a uniformly reduction of electric field strength and thus the band gap.

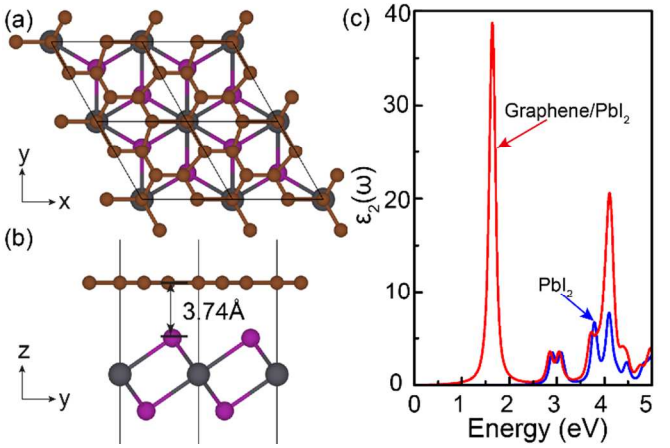

FIG. 6. (color online) (a) Top and (b) side views of the graphene/PbI_2 supercell, which corresponds to a $\sqrt{3}\times\sqrt{3}$ graphene cell and a 1×1 PbI_2 cell. (The light brown: carbon, grey: lead and purple: iodine). (c) The calculated imaginary part of the dielectric functions of monolayer PbI_2 (red solid line) and the hybrid graphene/PbI_2 (blue solid line) structure for the light incident in the c (z) direction and polarized along a/b (as indicted in Fig. 1) direction, respectively.

As shown above, the bandgap of PbI_2 monolayer is 2.63 eV which may only show marginal visible light absorption, but need to be further improved for developing potential application in optoelectronics and photovoltaics. Recent experiments[69-72] have shown that the combination of highly conductive graphene and optically active molybdenum disulphide (MoS_2) into a new family of 2D van der Waals (vdW) hetero-structure can photo-excite electron-hole pairs within MoS_2's band-gap, allowing achieving enhanced photocurrent in the visible light region. Carbon nanotube encapsulated within single layer PbI_2 nanotube has been fabricated in most recent experiment.[39] One intrigue question is whether the experimentally realized nanohybrid between carbon and PbI_2 can enhance the visible light response. To explore this, we have carried out systematic studies on the optical property of 2D graphene/PbI_2 vdW hetero-structure (G/PbI_2) to compare with a pure PbI_2 monolayer using state-of-the-art hybrid functional method. A $\sqrt{3}\times\sqrt{3}$ Graphene cell and a 1×1 PbI_2 cell were adopted to simulate the hybridized structure with a lattice mismatch of 8%. Note that we have kept the lattice vector of monolayer PbI_2 fixed and the lattice constant of graphene is elongated to match the substrate PbI_2. It should be noted that such a mismatch is not expected to affect our conclusion because graphene can sustain tensile stress as large as 20% with gapless gap maintained[73,74]. Fig. 6 (a) illustrates the optimized crystal structure of 2D vdW G/PbI_2 nanohybrid. The distance between monolayer PbI_2 and graphene is calculated to be 3.74 Å. In Fig. 6b, we present the calculated the imaginary part of the dielectric function for a pure PbI2 monolayer and the hybrid G/PbI_2 complex, respectively. Indeed the pure PbI_2 monolayer only shows marginal adsorption of visible light. However the 2D vdW G/PbI_2 heterostructure displays the enhanced visible light absorption and the red light shift of absorption edge is as large as 1.5 eV compared to that in a pure monolayer PbI_2. Since G/PbI_2 nano-hybrid has been realized in recent experiment[39], our finding highlight an interesting material for potential application in building novel 2D photonics and photovoltaic devices.

Conclusions

We have systematically studied the structure, stability, electronic and optical properties, and the effect of strain and spin-orbital-coupling in monolayer PbI_2 using the first principle method. Our phonon dispersion calculation confirms the dynamic stability of monolayer PbI_2 nanosheet. Spin-orbit interaction proves to be significant for monolayer PbI_2 and will give rise to a band gap reduction of 0.72 eV. Compared to the standard PBE functional, the electronic structure calculation with screened hybrid functional (HSE06) and the inclusion of spin-orbit coupling effect predicts not only an accurate band gap (2.63 eV), but also the correct energy level positon for CBM and VBM. Furthermore, biaxial strain can significantly tune the band gap of monolayer PbI_2 from 1 eV to 3 eV. Most interestingly, interfacing electrically active graphene with single layer PbI_2 nanosheet to form a 2D vdw type hetero-structure can substantially enhance the visible light response, suggesting potential applications of vdw nanohybrid in novel 2D optoelectronics and photovoltaics.

Acknowledgements

This work was supported by the Ministry of Science and Technology of China (Grant Nos. 2011CB606405 and 2011CB921901) and the National Natural Science Foundation of China (Grant No. 11334006). M.Z and A.D acknowledge generous grants of high-performance computer time from computing facility at Queensland University of Technology and Australian National Facility. A.D. greatly appreciates the Australian Research Council QEII Fellowship and financial support of the Australian Research Council under Discovery Project (DP130102420).

Notes and references

[a] Department of Physics and State Key Laboratory of Low-Dimensional Quantum Physics, Tsinghua University, Beijing 100084, China
[b] Institute for Frontier Materials, Deakin University, Waurn Ponds, VIC 3216, Australia
[c] School of Chemistry, Physics and Mechanical Engineering, Queensland University of Technology, Brisbane, QLD 4001, Australia.
[d]Collaborative Innovation Center of Quantum Matter, Tsinghua University, Beijing 100084, China.
*Corresponding Authors: Wenhui Duan: dwh@phys.tsinghua.edu.cn and Aijun Du: aijun.du@qut.edu.au

1 K. S. Novoselov, A. K. Geim et al., *Nature (London)*, 2005, **438**, 197; A. K. Geim, *Science*, 2009, **324**, 1530; A. K. Geim and K. S. Novoselov, *Nature Mater.* ,2007, **6**, 183.
2 S. Cahangirov, M. Topsakal, E. Aktürk, H. Sahin, and S. Ciraci, *Phys. Rev. Lett.*, 2009, **102**, 236804.
3 P. Vogt , P. De Padova , C. Quaresima , J. Avila , E. Frantzeskakis , M. C. Asensio , A. Resta , B. Ealet , G. Le Lay , *Phys. Rev. Lett.* , 2012 , **108** , 155501 .
4 Z. Ni, Q. Liu, K. Tang, J. Zheng, J. Zhou, R. Qin, Zh. Gao, D. Yu, and J. Lu, *Nano Lett.* ,2012, **12**, 113.
5 H. Sahin, S. Cahangirov, M. Topsakal, E. Bekaroglu, E. Aktürk, R. T. Senger, and S. Ciraci, *Phys. Rev. B*, 2009, **80**, 155453.
6 E. Bianco, S. Butler, S. Jiang, O. D. Restrepo, W. Windl, and J. E. Goldberger, *ACS Nano.* , 2013, **7**, 4414.
7 K. Watanabe, T. Taniguchi and H. Kanda, *Nat Mater.* 2004,**3**, 404.
8 J. N. Coleman, M. Lotya, A. O'Neill, S. D. Bergin, P. J. King, U. Khan, K. Young, A. Gaucher, S. De and R. J. Smith et al. *Science,* 2011, **331**, 568– 571.
9 M. Chhowalla, H. S. Shin, G. Eda, L. J. Li, K. Loh and H. Zhang, *Nat. Chem.*, 2013, **5**, 263.
10 Q. H. Wang, K. Kalantar-Zadeh, A. Kis, J. N. Coleman & M. S. Strano, *Nature Nanotechnology* ,2012, **7**, 699.
11 L. Li, Y. Yu, G. J. Ye, Q. Ge, X. Ou, H. Wu, D. Feng, X. H. Chen and Y. Zhang, *Nat. Nanotechnol.*, 2014, **9**, 372–377.
12 S. Das Sarma, S. Adam, E. H. Hwang, E. Rossi, *Rev. Mod. Phys.* 2011, **83**, 407.
13 B. Radisavljevic, A. Radenovic, J. Brivio, V. Giacometti, and A. Kis, *Nat. Nanotechnol.*, 2011, **6,** 147.
14 A. Splendiani, L. Sun, Y. Zhang, T. Li, J. Kim, C.-Y. Chim, G. Galli, and F. Wang, *Nano Lett.*, 2010,**10**, 1271.
15 D. Jariwala, V. K. Sangwan, L. J. Lauhon, T. J. Marks, M. C. Hersam, *ACS Nano.*, 2014, **8**, 1102– 1120.
16 C. R. Dean, A. F. Young, I. Meric, C. Lee, L. Wang, S. Sorgenfrei, K. Watanabe, T. Taniguchi, P. Kim, K. L. Shepard and J. Hone, *Nat. Nanotechnol.* 2010, **82**, 722– 726.
17 A. K. Geim, I. V. Grigorieva, *Nature,* 2013, **499**, 419– 425.
18 E. Flahaut, J. Sloan, S. Friedrichs, A. I. Kirkland, K. S. Coleman, V. C. Williams, N. Hanson, J. L. Hutchison and M. L. H. Green, *Chem. Mater.*, 2006, **18**, 2059−2069.
19 E. K. H. Salje, B. Palosz and B. Wruck, *J. Phys. C: Solid State Phys.*,1987, 20, 4077.
20 B. Palosz, W. Steurer and H. Schulz,*J. Phys.: Condens. Matter*, 1990, **2**, 5285.
21 A. E. Dugan and H. K. Henisch, *Phys. Rev.*,1968, **171**, 1047.
22 Ch. Gähwiller and G. Harbeke, *Phys. Rev.*,1969, **185**, 1141.
23 D. Blossey, *Phys. Rev. B*, 1971, **3**, 1382.
24 J. B. Anthony and A. D. Brothers, *Phys. Rev. B*,1973, **7**, 1539.
25 J. H. Beaumont, A. J. Bourdillon, and J. Bordas, J. Phys. C, *1977*, **10**, 761.
26 R. Ahuja, H. Arwin, A. Ferreira da Silva, C. Persson, J. M. Osorio-Guillen, J. Souza de Almeida, C. Moyses Araujo, E. Veje, N. Veissid, C. Y. An, I. Pepe and B. Johansson, *J. Appl. Phys.*, 2002, **92**, 7219.
27 M.R. Squillante and G. Entine, *Nucl. Instr. and Meth. A*, 1996, **380**, 160.
28 D.S. McGregor and H. Harmon, *Nucl. Instr. and Meth. A,* 1997, **395**, 101.
29 S. O. Kasap and J. A. Rowlands, *J. Mater. Sci., Mater. Electron.*, 2000, **11**,179.
30 M. M. Lee, J. Teuscher, T. Miyasaka, T. N. Murakami and H. J. Snaith , *Science*, 2012, **338**, 643– 647.
31 J. Y. Jeng, Y. F. Chiang, M. H. Lee, S. R. Peng, T. F. Guo, P. Chen and T. C. Wen, *Adv. Mater.*,2013, **25**, 3727.
32 Z. K. Tan, R. S. Moghaddam, M. L. Lai, P. Docampo, R. Higler, F. Deschler, M. Price, A. Sadhanala, L. M. Pazos, D. Credgington, et al., *Nat. Nanotechnol.* , 2014, **9**, 687– 692.

33 Green, M. A.; A. Ho-Baillie, H. J. Snaith, *Nat. Photonics*, 2014, **8**, 506– 514.
34 R. R. Meyer, J. Sloan, R. E. Dunin-Borkowski, A. I. Kirkland, M. C. Novotny, S. R. Bailey, J. L. Hutchison and M. L. H. Green, *Science*, 2000, **289**, 1324.
35 G. K. Kasi, N. R. Dollahon, and T. S. Ahmadi, *J. Phys. D: Appl. Phys.*,2007, **40**, 1778.
36 R. Kreizman, S. Y. Hong, J. Sloan, R. Popovitz-Biro, A. Albu-Yaron, G. Tobias, B. Ballesteros, B. G. Davis, M. L. H. Green and R. Tenne, *Angew.Chem., Int. Ed.*, 2009, **48**, 1230.
37 R. Kreizman, A. N. Enyashin, F. L. Deepak, A. Albu-Yaron, R. Popovitz-Biro, G. Seifert, R. Tenne, *Adv. Funct. Mater*. 2010, **20**, 2459– 2468.
38 Y. Z. Liu, C. H. Hu, A. Comotti and M. D. Ward, *Science,* 2011, **333**, 436.
39 L. Cabana, E. Batista, B. Ballesteros, C. Magén , R. Arenal , J. Oró-Solé , R. Rurali , and G. Tobias, *Adv. Mater.*, 2014, **26**, 2016–2021
40 C. Si, Z. Liu, W. Duan, and F. Liu, *Phys. Rev. Lett.*, 2013, **111**, 196802.
41 L. Kou, A. Du, T. Frauenheim and C. Chen, *Nanoscale*, 2014, **6**, 5156– 5161
42 Di Sante, D.; Stroppa, A.; Barone, P.; Whangbo, M.-H.; Picozzi, S.*, Phys. Rev. B, 2015,***91**, 161401(R)
43 G. Kresse and J. Furthmuller, *Phys. Rev. B*,1996, **54**, 11169.
44 G. Kresse and J. Furthmuller, *Comput. Mater. Sci.*,1996, **6**, 15.
45 J. P. Perdew, K. Burke, and M. Ernzerhof, *Phys. Rev. Lett.*, 1996, **77**,3865.
46 P. E. Blochl, *Phys. Rev. B*, 1994, **50**, 17953 .
47 G. Kresse and D. Joubert, *Phys. Rev. B,*1999, **59**, 1758.
48 J. Heyd, G. E. Scuseria, and M. Ernzerhof, J. *Chem. Phys.*, 2003, **118**, 8207.
49 J. Heyd, G. E. Scuseria, and M. Ernzerhof, *J. Chem. Phys.*, 2006, **124**, 219906.
50 L. J. Sham and M. Schlüter, *Phys. Rev. B,* 1985, **32**(6): 3883.
51 L. J. Sham and M. Schlüter. *Phys. Rev. Lett.,* 1983, **51**(20): 1888.
52 P. Mori-Sánchez, A. J. Cohen and W. Yang, *Phys. Rev. Lett.*, 2008, **100**(14): 146401.
53 A. J. Cohen, P. Mori-Sánchez and W. Yang, *Science,* 2008, **321**(5890): 792-794.
54 A. Togo, F. Oba, and I. Tanaka, *Phys. Rev. B*, 2008,**78**,134106.
55 S. Grimme, J. Antony, S. Ehrlich and H. Krieg, *J. Chem. Phys.*, 2010**,** ***132*** **(15),** 154104.
56 M. Gajdoš, K. Hummer, G. Kresse, J. Furthmüller, and F. Bechstedt, Phys. Rev. B, 2006**,** **73**, 045112.
57 I. Ch. Schluter and M. Schluter, *Phys. Rev. B* , 1974, **9,** 1652.
58 J. Robertson, *J. Phys. C* , 1979, **12**, 4753.
59 J. Robertson, *Solid State Commun.*, 1979, **12**, 4753.
60 J. R. Anderson and A. V. Gold, *Phys. Rev.,* 1965, **139**(5A): A1459.
61 A. B. Alekseyev, H. P. Liebermann and R. J. Buenker et al, *J. Chem. Phys.*, 2000, **113(4)**: 1514-1523.
62 M.H. Du, *J. Phys. Chem. Letts*., 2015, **6**, 1461.
63 B. Radisavljevic, A. Radenovic, J. Brivio. V. Giacometti and A. Kis, *Nature Nanotech*. 2011**, 6,** (3), 147-150.
64 S. W. Lee S W and S. K. Joo. *Electron Device Letters,* IEEE, 1996, **17(4)**: 160-162.
65 C. Lee, X. Wei, J. W. Kysar, et al. *Science,* 2008, **321**(5887): 385-388.
66 S. Bertolazzi, J. Brivio, and A. Kis, *ACS Nano.,* 2011*,* **5**, 9703-9709.
67 D. Akinwande, N. Petrone and J. Hone, *Nat. Commun*., 2014, **5**, 5678.
68 M. R. Tubbs, *Proc. R. Soc. Lond. A* 1964, **280**, 566.
69 K. Roy, M. Padmanabhan, S. Goswami, T. P. Sai, G. Ramalingam, S. Raghavan and A. Ghosh, *Nat. Nanotechnol*, 2013, **8**, 826-830.
70 J.M. Hamm and O. Hess, *Science,* 2013, **340**, 1298.
71 L. Britnell, R.M. Ribeiro, A. Eckmann, R. Jalil, B.D. Belle, A. Mishchenko, Y.J. Kim, R.V. Gorbachev, T. Georgiou *et al*., *Science*, 2013, **340**, 1311.
72 T. Georgiou, R. Jalil, B. D. Belle, L. Britnell, R. V. Gorbachev, S. V. Morozov, Y-J. Kim, A. Gholinia, S. J. Haigh and O. Makarovsky. et al. *Nat. Nanotech*. 2013, **8**, 100– 103
73 C. A. Marianetti1 and H. G. Yevick2, *Phys. Rev. Letts*., 2010, **105**, 245502.
74 V. M. Pereira, A. H. Castro Neto and N. M. R.Peres, *Physical Review B* 2009**, 80**, (4), 045401

